

Independent Component Analysis of Skin Color Image

Norimichi Tsumura, Hideaki Haneishi and Yoichi Miyake
Department of Information and Image Sciences,
Chiba University, Japan

Abstract

The spatial distributions of melanin and hemoglobin in human skin are separated by independent component analysis of skin color image. It is our goal to apply these results for the estimation of preferred skin color in color reproduction and the evaluation of a face browned by the sun and diagnosis of a skin disease. In this paper, the principle of independent component analysis is described and it is also shown that the components of melanin and hemoglobin from skin color image can be separated both theoretically and experimentally.

Introduction

It has been considered that the skin color reproduction is the most important problem for color reproduction of color film and color television systems.¹ With the recent progress of various imaging systems²⁻⁵ such as multi-media, computer graphic and telemedicine systems, the skin color becomes increasingly important for communication, image reproduction on hardcopy and softcopy, medical diagnosis, cosmetic development and so on.

Human skin is the turbid media with multi-layered structure.^{6,7} Various pigments such as melanin and hemoglobin are contained in the media. The slight changes of the structure and pigment construction produce rich skin color variation.⁸ Therefore, it is necessary to analyze the skin color based on the structure and pigment construction in reproducing and diagnosing the various skin colors.

In this research,²⁰ the spatial distributions of melanin and hemoglobin in skin are separated by independent component analysis of skin color image. The independent component analysis(ICA) is a technique that extracts the original signals from mixtures of many independent sources without a priori information on the sources and the process of the mixture. The ICA has been applied to the various problems such as array processing, communication, medical signal processing, and speech processing.⁹ In the field of color image processing, Inoue et al.¹⁰ proposed a technique to separate each pigment from compound color images. However, they could not obtain any practical result, since they assumed the linearity among the quantities of pigments and observed color signals in the intensity domain. In the intensity domain, generally, this linearity will not hold in practical applications. We improve their technique by

processing the color signals in the density domain, and apply it to the skin color image.

Independent Component Analysis

The ICA applied to the color image separation¹⁰ is described. Simplifying the description, we assume that the media is constructed by two pigments and that it is captured by an imaging system with two color channels. This simplification does not prevent the generalization of the problem except when the number of pigments is larger than the number of channels. This is discussed later in this section.

Let $x_{l,m}(1)$ and $x_{l,m}(2)$ denote the quantity of the two pigments on the coordinate (l,m) in the digital color image, $\mathbf{a}(1)$ and $\mathbf{a}(2)$ denote pure color vectors of the two pigments per unit quantity, respectively. Inoue et al. Assumed $\mathbf{a}(1)$ and $\mathbf{a}(2)$ are different from each other. They also assumed the compound color vector $\mathbf{e}_{l,m}$ on the image coordinate (l,m) can be calculated by the linear combination of pure color vectors with the quantities of $x_{l,m}(1)$ and $x_{l,m}(2)$ as

$$\mathbf{e}_{l,m} = \mathbf{A} \mathbf{x}_{l,m}, \quad (1)$$

where, $\mathbf{A} = [\mathbf{a}(1), \mathbf{a}(2)]$, $\mathbf{x}_{l,m} = [x_{l,m}(1), x_{l,m}(2)]^t$.

Each element of the color vector indicates the pixel value of each channel. Inoue et al. also assumed that the elements $x_{l,m}(1)$ and $x_{l,m}(2)$ of the quantity vector are mutually independent for the image coordinate (l,m) . Figures 1(a) and (b) show the process of the mixture and an example of probability density distribution of $x_{l,m}(1)$ and $x_{l,m}(2)$ that are mutually independent. Figure 1(c) shows the probability density distribution of $e_{l,m}(1)$ and $e_{l,m}(2)$ in the image, which are elements of compound color vector $\mathbf{e}_{l,m}$. It should be noted that the observed color signals $e_{l,m}(1)$ and $e_{l,m}(2)$ are not mutually independent. In Fig. 1(c), pure color vectors $\mathbf{a}(1)$ and $\mathbf{a}(2)$ are also shown to illustrate the relationship among the parameters.

By applying the ICA to the compound color vectors in the image, the relative quantity and pure color vector of each pigment are extracted without a priori information on the quantity and color vector under the assumption that quantities of pigments are mutually independent for the image coordinate. Let define the following equation using the separating matrix \mathbf{H} and separated vector $\mathbf{s}_{l,m}$ as shown in Fig. 1(a).

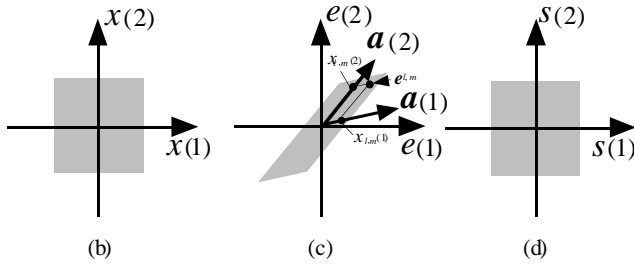
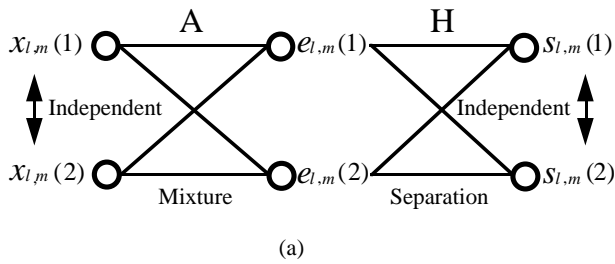


Figure 1. Mixture and separation of independent signals; (a) flow of the signals, (b) an example of probability density distribution of $x_{l,m}(1)$ and $x_{l,m}(2)$, (c) $e_{l,m}(1)$ and $e_{l,m}(2)$, and (d) $s_{l,m}(1)$ and $s_{l,m}(2)$.

$$s_{l,m} = H e_{l,m}, \quad (2)$$

where,

$$H = [h(1), h(2)], \quad s_{l,m} = [s_{l,m}(1), s_{l,m}(2)]^T,$$

and $h(1)$ and $h(2)$ are separating vectors. By finding the appropriate separating matrix H, we can extract the mutually independent signals $s_{l,m}(1)$ and $s_{l,m}(2)$ from the compound color vectors in the image. Many methods are proposed to find the separating matrix H (for example Ref. 11-15), such as using learning ability of artificial neural network,¹⁴ optimization techniques based on fixed point method.¹²

The extracted independent signals $s_{l,m}(1)$ and $s_{l,m}(2)$ may correspond to $x_{l,m}(2)$ and $x_{l,m}(1)$, respectively, and it is impossible to determine the absolute quantities $x_{l,m}(1)$ and $x_{l,m}(2)$ without an additional assumption. Therefore the extracted independent vector $s_{l,m}$ is given by

$$s_{l,m} = R \Sigma x_{l,m}, \quad (3)$$

where R is the permutation matrix that may substitute the elements of the vector each other, S is the diagonal matrix to relate the absolute quantities to relative qualities. Substituting Eqs. (1) and (2) into Eq. (3) gives

$$H A x_{l,m} = R \Sigma x_{l,m}. \quad (4)$$

Holding Eq. (4) in the arbitrary quantity vector, the matrix HA should be equal to the matrix RS, and the mixing matrix A is calculated by using the inverse matrix of H as follows:

$$A = H^{-1} R \Sigma. \quad (5)$$

Note that what we can obtain by the ICA are relative quantities and directions of compound color vectors. In our application of color image separation and synthesis, however, the absolute values are not required.

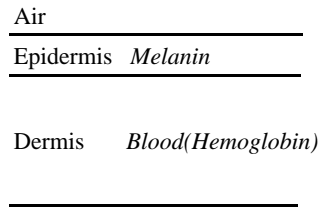


Figure 2. Schematic model of human skin with plane parallel epidermal and dermal layers

Figure 3. The analyzed skin color image with 64 x 64 pixels

If the number of pigments is larger than the number of channels, it is impossible to extract the independent components caused by reduction of the signals. On the other hand, if the number of pigments is smaller than the number of channels, it is possible to make the number of channels equal to the number of pigments by using the principal component analysis.^{14,16} This technique is also used in our analysis.

Skin Color Model

Schematic model of human skin is shown in Fig. 2 with plane parallel epidermal and dermal layers. The epidermal and dermal layers are the turbid media. Various pigments such as melanin, hemoglobin, bilirubin, and β -carotene are contained in the layers, especially melanin and hemoglobin are dominantly contained in the epidermal and dermal layer, respectively.

Figure 3 shows skin color image with 64×64 pixels used for the ICA. The image is extracted from the forehead of the facial image with 300×450 pixels taken by HDTV camera (Nikon HQ1500C) with 1920×1035 pixels. Each pixel of color images has three channels; red, green and blue. Let $r_{l,m}$, $g_{l,m}$, $b_{l,m}$ be the pixel values in red, green and blue channels of the skin color image on the image coordinate (l,m) , respectively.

Analyzing the above skin color, we made four assumptions on skin color. First, Lambert-Beer law or modified Lambert-Beer law¹⁷ holds in the reflected light among the quantities and observed color signals. Second, spectral distribution of the skin is not abrupt in the sensitive spectral range of each channel in the imaging system. Third, the spatial variations of color in the skin are caused by two pigments; melanin and hemoglobin. Fourth, these quantities are mutually independent spatially.

The first assumption assures the linearity among the observed color signals and pure color signals of pigments in the spectral density domain. In the optical density domain of three channels; $-\log(r_{l,m})$, $-\log(g_{l,m})$ and $-\log(b_{l,m})$, the linearity is assured by including the second assumption. On the basis of the linearity and the third assumption, the color in skin image is modeled as Fig. 4 in the optical density domain of three channels. It is seen that the three densities of skin color are distributed on the two dimensional plane spanned by pure color vectors of melanin and hemoglobin. Denote by $c_{l,m}$ color density vector on image coordinate (l,m) as

$$\mathbf{c}_{l,m} = [-\log(r_{l,m}), -\log(g_{l,m}), -\log(b_{l,m})]^T, \quad (6)$$

where $[\bullet]^T$ represents transposition. According to the skin color model shown in Fig. 4, the color density vector of skin can be expressed by

$$\mathbf{c}_{l,m} = \mathbf{C} \mathbf{q}_{l,m} + \mathbf{c}^{(3)}, \quad (7)$$

where

$$\mathbf{C} = [\mathbf{c}^{(1)}, \mathbf{c}^{(2)}], \quad \mathbf{q}_{l,m} = [q_{l,m}(1), q_{l,m}(2)]^T,$$

and $\mathbf{c}^{(1)}$ and $\mathbf{c}^{(2)}$ are pure density vectors of hemoglobin and melanin (or melanin and hemoglobin), $q_{l,m}(1)$ and $q_{l,m}(2)$ are relative quantities of the pigments respectively, $\mathbf{c}^{(3)}$ is spatially stationary vector caused by other pigments and skin structure. The vectors $\mathbf{c}^{(1)}$ and $\mathbf{c}^{(2)}$ are normalized as $\|\mathbf{c}^{(1)}\| = \|\mathbf{c}^{(2)}\| = 1$, where $\|\cdot\|$ is the Euclidean norm.

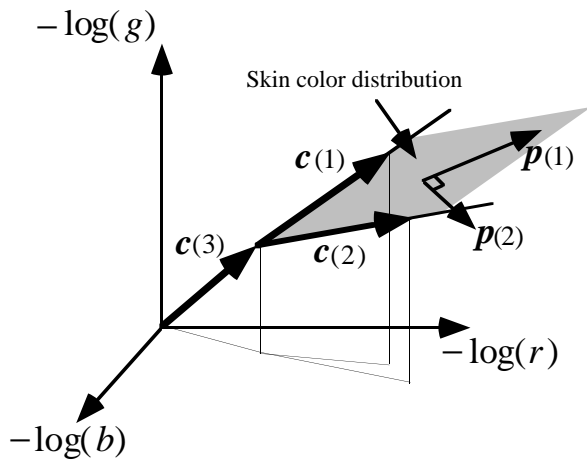


Figure 4. Skin color model in the optical density domain of three channels

It is easily understood that the ICA described in the previous section can be applied in the two dimensional plane spanned by $\mathbf{c}^{(1)}$ and $\mathbf{c}^{(2)}$ to estimate the quantity vector $\mathbf{q}_{l,m}$ from color density vectors $\mathbf{c}_{l,m}$. Principal component analysis (PCA) is used to extract the two-dimensional plane. The values of three channels can be adequately described by using the two principal components with the accuracy of 99.3%. Let denote the first, second and third principal component vectors as $\mathbf{p}^{(1)}$, $\mathbf{p}^{(2)}$ and $\mathbf{p}^{(3)}$, respectively. It is noted that $\mathbf{p}^{(1)}$, $\mathbf{p}^{(2)}$ will span the two dimensional space spanned by $\mathbf{c}^{(1)}$ and $\mathbf{c}^{(2)}$.

Here define a projection matrix $\mathbf{P} = [\mathbf{p}^{(1)}, \mathbf{p}^{(2)}] [\mathbf{p}^{(1)}, \mathbf{p}^{(2)}]^T$ onto the two dimensional space spanned by $\mathbf{c}^{(1)}$ and $\mathbf{c}^{(2)}$. Based on the projection, the color density vector $\mathbf{c}_{l,m}$ can be divided into two components as follows:

$$\mathbf{c}_{l,m} = \mathbf{P} \mathbf{P}^T \{ \mathbf{C} \mathbf{q}_{l,m} + \mathbf{c}^{(3)} \} + (\mathbf{I} - \mathbf{P} \mathbf{P}^T) \mathbf{c}^{(3)}, \quad (8)$$

where matrix \mathbf{I} denotes an identity matrix. The first term indicates the component in the two dimensional subspace spanned by $\mathbf{c}^{(1)}$ and $\mathbf{c}^{(2)}$ or $\mathbf{p}^{(1)}$ and $\mathbf{p}^{(2)}$. The second term indicates the component in the one dimensional subspace

which is spanned by $\mathbf{p}^{(3)}$.

Skin Color Image Separation

The skin color model proposed in the previous section is used to extract the unknown color density matrix \mathbf{C} and unknown relative quantity vectors $\mathbf{q}_{l,m}$ as follows.

Let us define the score vector $\mathbf{w}_{l,m}$ in the first term of Eq. (8) as

$$\mathbf{w}_{l,m} = \mathbf{P}^T \mathbf{C} \mathbf{q}'_{l,m} \quad (9)$$

where, $\mathbf{q}'_{l,m} = \mathbf{q}_{l,m} + (\mathbf{P}^T \mathbf{C})^{-1} \mathbf{P}^T \mathbf{c}^{(3)}$.

Making the task of ICA easier,^{14,16} the elements in score vector $\mathbf{w}_{l,m}$ were made zero mean by subtracting the mean vector $\bar{\mathbf{w}}$, and unit variance by multiplying the inverse square root of the 2×2 diagonal matrix $\mathbf{D} = \text{diag}[\lambda_{(1)}, \lambda_{(2)}]$, where $\lambda_{(1)}$ and $\lambda_{(2)}$ denote the eigenvalues for the first and second principal components respectively. The whitened vector denoted by $\mathbf{e}_{l,m}$ is written as

$$\mathbf{e}_{l,m} = \mathbf{D}^{-1/2} \mathbf{P}^T \mathbf{C} \mathbf{x}_{l,m}, \quad (10)$$

where, $\mathbf{x}_{l,m} = \mathbf{q}'_{l,m} - (\mathbf{P}^T \mathbf{C})^{-1} \bar{\mathbf{w}}$.

Here, we define $\mathbf{A} = \mathbf{D}^{-1/2} \mathbf{P}^T \mathbf{C}$, then we get Eq. (11) that is as same as Eq. (1).

$$\mathbf{e}_{l,m} = \mathbf{A} \mathbf{x}_{l,m} \quad (11)$$

The separation matrix \mathbf{H} is obtained by the ICA for the normalized vectors $\mathbf{e}_{l,m}$, and the mixing matrix is calculated by Eq. (5). Substituting the $\mathbf{A} = \mathbf{D}^{-1/2} \mathbf{P}^T \mathbf{C}$ into the Eq. (5) and solving for the color matrix \mathbf{C} , the estimated matrix $\tilde{\mathbf{C}}$ of pure color densities is calculated as,

$$\tilde{\mathbf{C}} = (\mathbf{D}^{-1/2} \mathbf{P}^T)^{-1} \mathbf{H}^{-1} \mathbf{R} \mathbf{\Sigma}. \quad (12)$$

The diagonal matrix $\mathbf{\Sigma}$ was decided to normalize the matrix $\tilde{\mathbf{C}}$ as $\|\mathbf{c}^{(1)}\| = \|\mathbf{c}^{(2)}\| = 1$, permutation matrix \mathbf{R} was an identity matrix in this paper.

Each element of separation matrix \mathbf{H} was obtained by minimizing the Burel's independence evaluation value¹¹ for the elements of vector $\mathbf{s}_{l,m}$. The independence evaluation value ranges from 0 to 1, and if the value is 0, the signals are mutually independent. The minimization is performed by quasi-Newton implementation using the MATLAB tool box.¹⁸ The independence evaluation values for the observed signals $\mathbf{e}_{l,m}(1)$, $\mathbf{e}_{l,m}(2)$ and resultant signals $\mathbf{s}_{l,m}(1)$, $\mathbf{s}_{l,m}(2)$ were 0.2414 and 0.0081, respectively. We can conclude that $\mathbf{s}_{l,m}(1)$ and $\mathbf{s}_{l,m}(2)$ are fairly independent of each other, therefore melanin and hemoglobin were distributed independently in the skin color image.

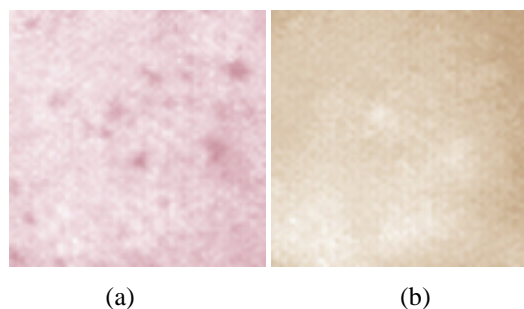


Figure 5. Separated two independent components of the skin color image; (a) first and (b) second independent components. The synthesis parameters are set as (a) $K = \text{diag}[1,0]$ and $j=0$, (b) $K = \text{diag}[0,1]$ and $j=0$.

Let define \tilde{C}^+ as the Moore-Penrose's generalized inverse matrix of \tilde{C} , and \mathbf{b} as $\min(\tilde{C}^+ \mathbf{c}_{l,m})$ assuming that the smallest value of each element in $\mathbf{q}_{l,m}$ in skin image is zero. The color separation and synthesis equation is written by

$$\mathbf{c}'_{l,m} = \tilde{C} \{K(\tilde{C}^+ \mathbf{c}_{l,m} - \mathbf{b}) + j\mathbf{b}\} + j(\mathbf{I} - \mathbf{P} \mathbf{P}^t) \mathbf{c}_{l,m}, \quad (13)$$

where $\mathbf{c}'_{l,m}$ is the synthesized color, K is the diagonal matrix to change the quantities of pigments $\mathbf{q}_{l,m}$, j is the value to change quantities of stationary color vector $\mathbf{c}_{(3)}$. We call the K and j synthesis parameters.

Figures 5 (a) and (b) show the separated two independent components; first and second independent components, respectively. We set the synthesis parameters as $K = \text{diag}[1,0]$ and $j=0$ in Fig. 5(a), $K = \text{diag}[0,1]$ and $j=0$ in Fig. 5(b). It is considered that the first and second independent components are caused by hemoglobin and melanin, respectively, since the pimples are appeared in the first independent component and not appeared in the second independent component.

Conclusion

The skin color image was separated into two images by independent component analysis in optical density domain of three color channels. We believe that the images correspond to distributions of the melanin and hemoglobin, respectively, because the result of separation agreed well with the physiological knowledge. The separated components can be synthesized to simulate the various facial color images by changing the quantities of the separated two pigments.

Acknowledgement

A part of this research was supported by Photographic Research Fund of Konica Imaging Foundation.

References

1. R. W. G. Hunt, *The reproduction of colour* (Fountain press, London, 1995).

2. F. H. Imai, N. Tsumura, H. Haneishi et al., "Principal component analysis of skin color and its application to colorimetric color reproduction on CRT display and hardcopy," *J. Image Sci. and Tech.* **40**, 422-430 (1996).
3. Y. Yokoyama, N. Tsumura, H. Haneishi, et al., "A new color management system based on human perception and its application to recording and reproduction of art printing," *IS&T/SID's 5th Color Imaging Conference* 169-172 (1997).
4. P. Hanarahan and W. Krueger, "Reflection from layered surfaces due to subsurface scattering," *Proc. SIGGRAPH 93* 165-174 (1993).
5. M. Yamaguchi, R. Iwama, Y. Ohya, et al., "Natural color reproduction in the television system for telemedicine," *Proc. SPIE* **3031**, 482-489 (1997).
6. M. M. C.van Gemert, S. L. Jacques, and H. J. C. M. Sternborg et al., "Skin optics," *IEEE Trans. Biomed. Eng.* **36**,1146-1154 (1989).
7. R. R. Anderson and J. A. Parrish, "The optics in human skin," *J. Invest. Dermatol.* **77**, 13-19 (1981).
8. E. A. Edwards and S. Q. Duntley, "The pigments and color of living human skin," *Am. J. Anat.* **65**, 1-33 (1939).
9. J. Karhunen, A. Hyvarinen, R. Vigário, et al., "Applications of neural blind separation to signal and image processing," *Proceedings of IEEE Int. Conf. on ASSP* **1**, 131-134 (1997).
10. T. Inoue, Y. Fujii, K. Itoh et al., "Independent component analysis for a small number of elements in high-dimensional space," *Proceedings of Japan Optics '95* 105-106 (1995). (in Japanese)
11. G. Burel, "Blind separation of sources: a nonlinear neural algorithm," *Neural Networks* **5**, 937-947 (1992).
12. A. Hyvärinen and E. Oja, "A fast fixed-point algorithm for independent component analysis," *Neural computation* **9**, 1483-1492 (1997).
13. C. Jutten and J. Hearult, "Blind separation of sources, Part I : An adaptive algorithm based on neuromimetic architecture," *Signal Processing* **24**, 1-10 (1991).
14. J. Karhunen, E. Oja, L. Wang, R. Vigário and J. Joutsalo, "A Class of Neural Networks for Independent Component Analysis," *IEEE Trans. Neural Network* **8**, 486-504 (1997).
15. H. H. Yang and S. Amari, "Adaptive online learning algorithms for blind separation: maximum entropy and minimum mutual information," *Neural computation* **9**, 1457-1482 (1997).
16. K. Shirasaki, T. Inoue, K. Itoh, et al., "Two-stage independent component analysis and its applications to extraction of original images from the mixtures," *Japanese Journal of Optics* **25**, 537-543 (1996). (in Japanese)
17. M. Hiraoka, M. Firbank, M. Essenpreis, et al, "A Monte Carlo investigation of optical pathlength in inhomogeneous tissue and its application to near-infrared spectroscopy," *Phy. Med. Biol.* **38**, 1859-1876(1993).
18. A. Garce. *Matlab Optimization Toolbox User's Guide* (The Math Works, Boston, MA, 1992).
19. P. J. Dwyer, R. R. Anderson and C. A. DiMarzio, "Mapping blood oxygen saturation using a multi-spectral imaging system," *Proc. SPIE* **2976**, 270-280 (1997).
20. N. Tsumura, H. Haneishi, Y. Miyake, "Independent component analysis of skin color image," *J. Opt. Soc. Am. A* (submitted).